Sparse repulsive coupling enhances synchronization in complex networks

I. Leyva, I. Sendiña-Nadal, J. A. Almendral, and M. A. F. Sanjuán
Departamento de Ciencias de la Naturaleza y Física Aplicada, Universidad Rey Juan Carlos, c/Tulipán s/n, 28933 Móstoles, Madrid, Spain
(Received 31 August 2006; published 20 November 2006)

Through the last years, different strategies to enhance synchronization in complex networks have been proposed. In this work, we show that synchronization of nonidentical dynamical units that are attractively coupled in a small-world network is strongly improved by just making phase-repulsive a tiny fraction of the couplings. By a purely topological analysis that does not depend on the dynamical model, we link the emerging dynamical behavior with the structural properties of the sparsely coupled repulsive network.

DOI: 10.1103/PhysRevE.74.056112 PACS number(s): 89.75.Fb, 05.45.Xt, 87.19.La

I. INTRODUCTION

After the seminal papers by Watts and Strogatz [1] and by Barabási and Albert [2], complex systems started to be described within the framework of complex networks. First, attention was focused on the structural and functional properties of such networks, being the most studied the small-world [3] (SW) and scale-free [4,5] ones as many natural (neural, genetic, chemical) and man-made (power grids, Internet, social networks) systems have been characterized with a similar underlying connectivity structure. Next, the interest was shifted to the implications on the global dynamical behavior of ensembles of nonlinear active units when they are coupled through a nontrivial scheme [6] instead of being organized in a lattice. Among the dynamical processes occurring on a network (see [7] for a review), such as pattern formation [8,9], spreading processes, or synchronization, the latter has captured more pages in the literature. Synchronous behavior is considered one of the mechanisms to transmit and code information in complex systems, ranging from neuronal assemblies [10] to networks of chemical oscillators of the Belousov-Zhabotinsky reaction [11,12] or social communities [13]. The interplay between the network structure and the dynamics of each interacting subsystem can provide stronger synchronizability or faster propagation of information [6].

Theoretically, the network propensity for synchronization was first tackled in [14]. Since then, several strategies have been developed with the aim of finding the best way to achieve synchronization in complex networks. These approaches have mainly focused on the role that weighted links play in networks with a heterogeneous degree distribution [15–17], on the importance of shortest paths and clustering in SW networks [10], and on the effect of the input degree regardless of the global structure [18]. Another recent approach, a kind of reverse engineering, consists in defining a recursive algorithm to build up a network with N nodes and a mean degree k which minimizes some synchronizability parameter [19].

Most of this research has been devoted to attractively coupled dynamical elements. However, it is known that biological networks combine different types of connections to improve synchronization and transmission performance, as in the case of the coexistence of excitatory and inhibitory synapses in the brain [20]. In [21] it was studied pattern formation in a two-dimensional (2D) array of oscillators with phase-shifted coupling, in particular for phase shift π, which corresponds to a repulsive coupling, while in [22] a chain of negatively coupled chaotic oscillators is compared to an experimental laser system with negative feedback and delay. Obviously, two attractively coupled oscillators tend to oscillate in phase whereas they do it in antiphase if repulsively coupled. Nevertheless, in complex networks, little attention has been paid to the effect of repulsive coupling or to the interaction between different types of coupling. The scarce literature addressing synchronization in repulsively coupled oscillators deals mainly with phase oscillators and considers either a lattice [23] or a fully connected topology [24], but the influence of the network structure is still an open question. In addition, almost all the published work on synchronization in complex networks is basically related to arrays of identical dynamical units. However, heterogeneity of elements is an inherent feature present in natural systems which can be especially relevant in the dynamics of biological networks.

In the present work, we explore the influence of the network topology on the dynamics of nonidentical coupled units, when a small fraction of the links is phase repulsive. In the following section, we first consider a chain of excitable and oscillatory units and show that sparse repulsive links in a SW structure can induce a coherent oscillatory state when the equivalent SW composed of only attractive connections is not able to synchronize or even to activate the heterogeneous ensemble. The effect of sparse repulsive couplings is also demonstrated in a simpler network of spinlike dynamical units in Sec. III. Then, just by means of an analysis focused on the eigenvalues of the connectivity matrix, we link the emerging dynamical behavior with the structural properties of the sparsely coupled repulsive network in Sec. IV.

II. NETWORK OF EXCITABLE AND OSCILLATORY ELEMENTS

In our study, we consider an ensemble of nonidentical Hodgkin-Huxley (HH) units [25] as the dynamical elements to be placed on each of the N nodes of our network. Although this model is an accurate biophysical description of a

neuron, it is chosen for this work as long as it is able to exhibit both excitable and oscillatory behavior. The cell model reads

$$CV_i = g_{Na}m_i^3h_i(V_{Na} - V_i) + g_K n_i^4(V_K - V_i) + g_l(V_l - V_i) + \frac{d}{k_i}\sum_{j=1}^{N} c_{ij}(V_j - V_i) + I_i, \tag{1a}$$

$$x_i = \alpha_x(1 - x_i) - \beta_x x_i, \tag{1b}$$

where V_i is the voltage variable of cell i and $x_i \in \{m_i, n_i, h_i\}$ are conductances. Parameter values and functions α_x and β_x are the standards in the literature [25,26]. I_i controls the dynamics of an isolated unit and is chosen as the control parameter to introduce heterogeneity in the population. We set I_i uniformly distributed within an interval $I_0 \pm \Delta I$ to obtain an ensemble of excitable and oscillatory units. The value $I_0=9$ is fixed close to the point where an inverse Hopf bifurcation occurs. This way, for the chosen $\Delta I=0.2$, we observe that about 70% of the elements stay around the silent state, while the rest oscillate with a frequency that depends on I_i, which is close to 70 Hz for the chosen parameter range.

The dynamical units are diffusively connected. The coupling structure in Eq. (1a) is given by the connectivity matrix $\mathbf{C}=(c_{ij})$, defined by $c_{ii}=0$, $c_{ij}=\pm 1$ if nodes i and j are connected and $c_{ij}=0$ otherwise. k_i normalizes the connection strength by the number of incoming links to node i, and the coefficient d stands for the global coupling strength. The positive sign in $\mathbf{C}$ stands for an attractive coupling whereas the negative sign does for a repulsive one. The coupling term in Eq. (1a) can be written as

$$\frac{d}{k_i}\sum_{j=1}^{N} c_{ij}(V_j - V_i) = d\sum_{j=1}^{N} \ell_{ij}V_j, \tag{2}$$

in which $\mathbf{L}=(\ell_{ij})$ is the Laplacian of the graph, being

$$\ell_{ii} = -\frac{1}{k_i}\sum_{j=1}^{N} c_{ij} \quad \ell_{ij} = \frac{c_{ij}}{k_i}. \tag{3}$$

A. Local coupling

Initially we consider the dynamics of an ensemble of N elements on a one-dimensional array locally coupled for both fully phase-attractive and phase-repulsive coupling. The resulting connectivity matrix becomes $c_{i,i\pm1}=+1$ for the locally attractive coupling scheme, $c_{i,i\pm1}=-1$ in case of purely repulsive coupling, and $c_{ij}=0$ otherwise. The system given by Eq. (1) is numerically integrated using a fourth-order Runge-Kutta method with time step $\Delta t=0.05$ and free-boundary conditions.

To study the frequency synchronization process of the heterogeneous chain of active elements with the coupling strength, we calculate the global mean frequency of oscillation (MF) and its standard deviation σ_{MF}. MF is the average of the frequencies of the N elements in the array. The frequency of an element is determined by counting the number of spike events that occur in a unit time. A small σ_{MF} means that all elements are oscillating at the same rate, which is given by MF, and a large σ_{MF} reflects that many elements are silent, resulting in a MF much lower than the frequency of an oscillating element.

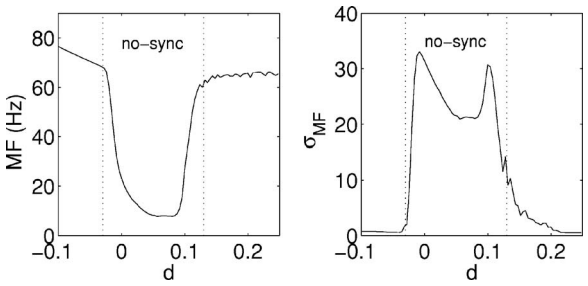

FIG. 1. Mean frequency of oscillation (MF) (left) and its standard deviation σ_{MF} (right) for an array of $N=400$ locally coupled HH units as a function of the coupling strength d, each point averaged over 100 realizations. The negative sign of d corresponds to the phase-repulsive scheme.

In Fig. 1 we plot MF and σ_{MF} as a function of d ranging from negative to positive values. Note that we can treat simultaneously both attractive and repulsive coupling schemes because the difference between the connectivity matrices is just a minus sign which is introduced into d. When $d>0$ is large enough, the system is frequency entrained (i.e., $\sigma_{\mathrm{MF}} \approx 0$) and synchronized with a linear phase distribution (not shown). Equivalently, for a sufficient $d<0$, the system is also frequency synchronized and reaches an antiphase synchronization state. It can be noted from Fig. 1 that the entrainment with negative couplings is achieved for smaller absolute values of d compared to the case with positive ones. This indicates that a phase-repulsive coupling is more effective in activating and entraining the whole network. Many biological systems exhibit this kind of repulsive coupling when their dynamical units are in competition with each other. Known examples are the inhibitory coupling present in neuronal circuits associated with a synchronized behavior in central pattern generators [27] or calcium oscillations in epileptic human astrocyte cultures [28].

B. Nonlocal random coupling

Our main interest is to explore the influence of a SW-like connection topology in the activation and synchronization of the network as the repulsive couplings are varied. From the results obtained in the previous section, we know that a small positive coupling strength is less efficient than a negative one to activate and synchronize the whole array when the units are locally coupled. Taking this into account, we consider now the possibility of both attractive and repulsive nonlocal links. The global coupling strength is fixed to $d=0.1$—i.e., within the unsynchronized regime for local positive coupling as shown in Fig. 1. The coupling matrix $\mathbf{C}$ is modeled now by keeping the local connections positive, $c_{i,i\pm1}=+1$, and by randomly adding (rather than rewiring [29]) a fraction p of the $(N-1)(N-2)/2$ possible long-range links, being negative with probability q. That is, since $p \in [0,1]$ is the probability of having a long-range connection, $c_{ij} \neq 0$ with $|i-j|>1$, we

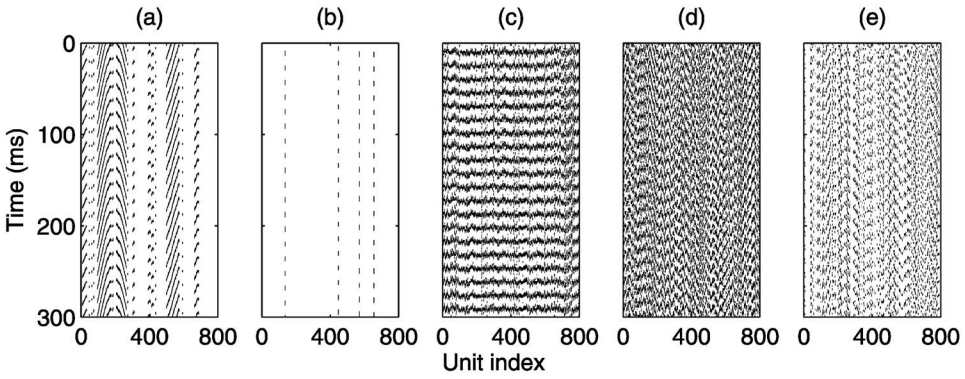

FIG. 2. Space-time plots of the voltage variable for a $N=800$ HH units network, with $\Delta I=0.2$, $d=0.1$, and different coupling schemes. (a) Attractive local coupling, $p=0$. (b)–(e) Network with long-range couplings: (b) purely attractive $p=0.0055$, $q=0$, and (c)–(e) partially repulsive: (c) $p=0.0055$, $q=0.3$, (d) $p=0.0055$, $q=0.45$, and (e) $p=0.015$, $q=0.3$.

have that $c_{ij}=-1$ with probability pq, and $c_{ij}=+1$ with probability $p(1-q)$.

Figure 2 shows space-time plots of the voltage variable through the whole array for different values of p and q. As expected, in the absence of long-range connections ($p=0$), few more than the initial 30% of the units are oscillating for the chosen coupling strength d; i.e., the array is not even activated as shown in Fig. 2(a). When long-range links are included, the first observation is that for any p, a minimum fraction of the new added links need to be repulsive ($q\neq 0$) in order to increase the activity of the network. This becomes evident when comparing Fig. 2(b) with Figs. 2(c)–2(e). In Fig. 2(b) the activity generated by the initially oscillating units is reduced, or even annihilated, when all long-range connections are attractive ($q=0$). However, the scenario completely changes when some of the shortcuts are repulsive ($q>0$) as in Figs. 2(c)–2(e), where self-sustained activity emerges for nonzero q. In addition, we observe that for certain probabilities p and q the collective oscillation becomes highly coherent [see Fig. 2(c)]. If we keep p fixed but q is increased the coherence is spoiled [Fig. 2(d)]. Likewise, coherence also worsens if q is the same as in Fig. 2(c) but p is different [Fig. 2(e)]. This is shown by comparing Fig. 2(c) with Fig. 2(d), in which p is the same as in Fig. 2(c) but q is higher.

To study quantitatively how the dynamics is affected by p and q, we measure the MF of the network and the standard deviation of the average activity, $V(t)=(1/N)\Sigma_{i=1}^{N}V_i(t)$, obtained as

$$\sigma_V=\sqrt{\overline{V^2}-\bar{V}^2},\quad \bar{V}=\langle V(t)\rangle_t,\quad \overline{V^2}=\langle V^2(t)\rangle_t, \tag{4}$$

where $\langle\cdots\rangle_t$ denotes temporal average. While the MF gives us an estimation of how much the network is activated, the σ_V defines how coherent the activity of the entire network is. If the network is fully activated, the MF approaches a rate of around 70 Hz, whereas σ_V is maximal if this activity is synchronized; that is, if all the units are oscillating at the same time, the average activity $V(t)$ is also oscillating and the deviation of this signal with respect to the mean value is higher than for an incoherent activity.

The effect of the topology in the dynamics can be seen in Fig. 3 as a function of the link probability p and the probability q of being repulsive, using contour plots and cross-section graphs. We first observe that there is a change in the behavior of both the activity and coherence as a function of p. The effect in the activity is shown in panels (a) and (c) through the MF and in the coherence of this activity in panels (b) and (d) through σ_V. While for the MF there is a

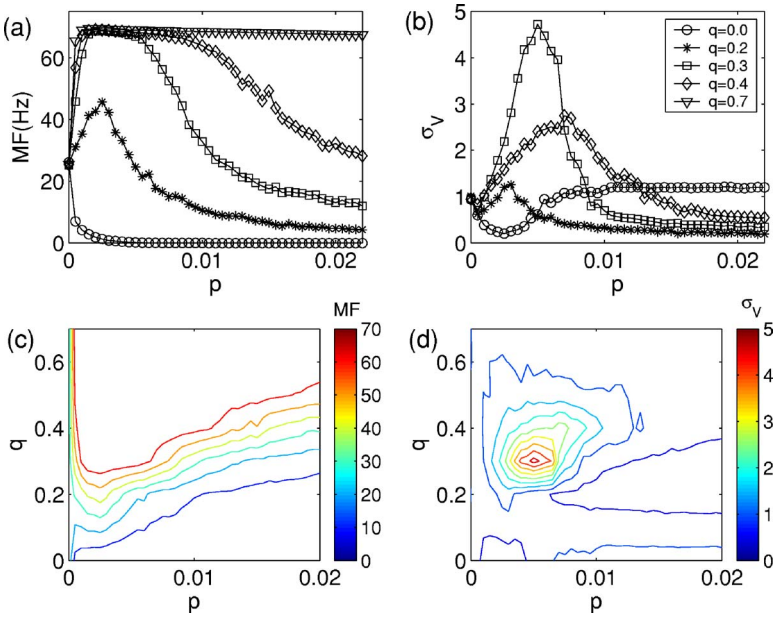

FIG. 3. (Color online) Mean frequency (MF) and network coherence σ_V as a function of p and q in a $N=800$ network. While panels (a) and (b) are cross sections of the 3D representation of MF and σ_V for several values of q, respectively, panels (c) and (d) are contour plots in the p-q plane. It becomes evident from panel (d) that there exist values for p and q for which the coherence is maximum. Each point is averaged over 100 simulations, 1 s long (transients avoided), for different network and initial conditions realizations. Legend in panel (b) applies also to panel (a).

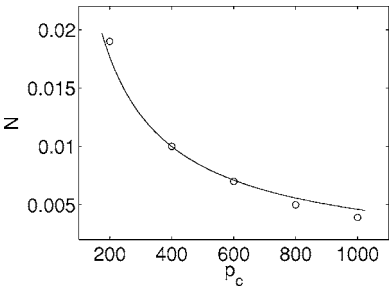

FIG. 4. Dependence of p_c on N, indicating that the emergence of coherent oscillations coincides with the birth of the GCC of a random network—i.e., $p_c \propto \ln(N)/N$. Here $q=0.25$.

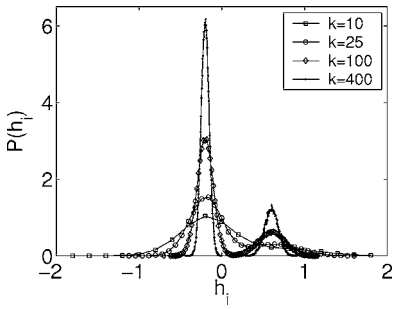

FIG. 5. Probability distribution of the input received by a node in the Ising model. Several node degrees k are shown for parameters $q=0.3$ and $r=0.25$.

transition towards a fully activated system at certain p, the σ_V reaches a maximum at this point.

When we explore the dependence of this special probability with the ensemble size, we find that it fits to $\ln(N)/N$ (see Fig. 4), which is the probability at which the giant connected component (GCC) of a Poisson random graph emerges, a well-known result in graph theory [7]. Precisely, the probability at which the global dynamics is more coherent coincides with the birth of the GCC of our network when only the randomly added long-range connections are considered (i.e., when the local couplings are neglected). Then, to reflect this "critical" transition, in what follows we refer to this special probability as p_c.

From Fig. 3 we can also observe the importance of q in the behavior of the MF and σ_V. First, it is clear that a value of $q \neq 0$ is needed to activate the network, since MF close to zero means that there are few dynamical units oscillating [panels (a) and (c)]. Second, the maximal activity is reached within an interval of p that depends on q. Note that this activity is not always coherent as panels (b) and (d) show. And finally, the signature of a network resonance, in both p and q, becomes manifest since coherence—i.e., σ_V—is maximally enhanced for the optimal values $p=p_c=0.0055$ and $q=0.3$. The probability p_c depends slightly on q, shifting to higher p as q increases, but remaining close to 0.0055.

III. ISING NETWORK

To analyze if the previous SW connectivity structure with long-range sparse repulsive links affects other dynamics imposed on it, we consider a discrete spinlike dynamics in which each node i has only two possible states $s_i=\pm 1$. This could model a social system with N agents choosing from two different opinions or in a biological context it could represent the firing state of a neuron. We prepare the system by setting rN of the spins at the state -1 and the rest at the opposite, r being the initial probability of finding a spin at -1. Consequently, with the same Laplacian matrix $\mathbf{L}$ introduced in Sec. II B, node i receives an input $h_i=\Sigma_j \ell_{ij} s_j \in [-2,2]$. Hence, as other authors have pointed out [3,30], these spinlike networks can be regarded as a pattern of the internal states and their evolution represent the global dynamics. Notice that the neighbor vertices linked repulsively contribute to the input with the opposite state. Then, in this model it is implicit that nodes linked with an attractive connection tend to follow the same evolution, whereas repulsive connection leads them to evolve differently.

We can prove analytically that the distribution of h_i presents two peaks: $\mu_1=-2r\sqrt{1-4q(1-q)}$ and $\mu_2=2(1-r)\sqrt{1-4q(1-q)}$ (see Fig. 5). Note that the position of these two peaks does not depend on the node degree k, thus neither does on the link probability p. Then, we choose to evolve the network according to the following local majority rule: the new state of node i is updated to $s_i(n+1)=+1$ if $h_i(n)>\mu_2$, $s_i(n+1)=-1$ if $h_i(n)<\mu_1$, and $s_i(n+1)=s_i(n)$ otherwise (i.e., the vertex keeps its state).

Using the same quantity defined by Eq. (4) to estimate the coherence of the output, we find that the system changes its behavior at $p \approx p_c$. This time σ_m measures the deviation of the global average state of the spin network after a transient. It can be seen in Fig. 6 that the maximum of σ_m is reached again when the GCC associated with the long-range links spans the whole network with a minimal number of links. Interestingly, a similar resonant trend with q is observed. This shows how p and q contribute to improve the synchronization even for this discrete dynamics.

IV. SPECTRAL ANALYSIS

Recently [14–17,31,32], the method of the *master stability function* [33] has been successfully used to analyze whether the network structure has some bearing on the dy-

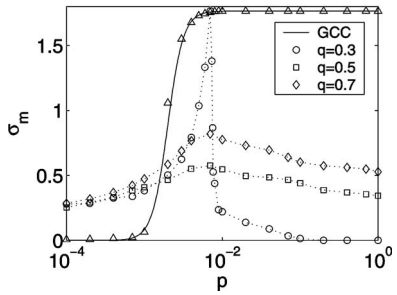

FIG. 6. Deviation σ_m of the global average state vs p for different q probabilities in a log-linear scale for $N=800$ spin network. Each point averages 1000 runs after a transient of 100 iterations and fixed $r=0.1$.

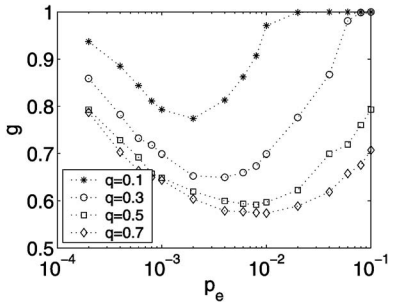

FIG. 7. Dependence of the structure parameter g with the adding link probability p, in a log-linear scale, for different probabilities q. Each point is an average over 100 different realizations of a $N=800$ network.

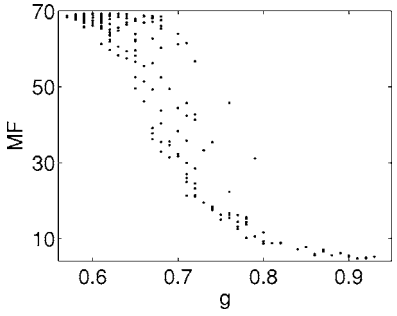

FIG. 8. Relationship between the mean frequency and the structure parameter g. MF comes from the numerical simulations and g is the parameter defined in the spectral analysis. Each point is the MF and g values corresponding to a pair (p,q).

namics evolving on it. However, this approach requires the dynamical units to be identical, which is not our case, and the use of the master stability function is not straightforward [17]. Hence, in order to understand the influence of a complex connectivity, we use a purely structural analysis based on the properties of $\mathbf{L}$. This is done by considering the impact of the spectra of $\mathbf{L}$ in the evolution of the term associated with the structure in Eq. (1). Notice that this impact can only be meaningful and relevant to the global dynamics if it occurs within the intrinsic dynamical time scale ($\tau \approx 15$ ms, since the MF≈ 70 Hz).

When we just consider $\dot{\mathbf{V}}=d\mathbf{L}\mathbf{V}$, where $\mathbf{V}=(V_1,\ldots,V_N)$, there is a basis in which $V_i \propto \exp(d\lambda_i t)$, where λ_i are the eigenvalues of $\mathbf{L}$. It is well known that all the eigenvalues of the Laplacian associated with a network with only attractive couplings are negative. However, when we add some repulsive connections, $\mathbf{L}$ has positive and negative eigenvalues [34]. We find that any set of initial states rapidly evolves into the subspace S^+ associated to the positive eigenvalues within a time smaller than the characteristic temporal scale of the system dynamics.

To quantify the effect of S^+, we note that, for a given positive λ_i^+, $e^{d\lambda_i^+}$ is a measure of how much the system spreads into the subspace defined by the corresponding eigenvector. Then, the ratio $e^{d\lambda_i^+ t}/e^{d\lambda_{\max} t}=e^{d(\lambda_i^+-\lambda_{\max})t}$ measures how different the evolution is in that subspace with respect to the one where the system develops faster. By defining the geometric average $g(t)=\prod_{i=1}^{N} e^{d(\lambda_i^+-\lambda_{\max})t/N}=e^{d(\langle\lambda^+\rangle-\lambda_{\max})t}$, we can estimate the homogeneity of the evolution in S^+ with a number in (0,1]. A value close to 1 means the system evolves similarly in all dimensions of S^+, whereas a low g implies that its behavior is affected by those vectors with the largest associated eigenvalues.

We are interested in the behavior of $g(t)$ as a function of p and q. As the shape of $g(t)$ is not very sensitive to time, we fix $t=d^{-1}\sim\tau$ to focus our study within the time scale of our dynamical unit. In Fig. 7 we observe that $g(\tau)$, in short g, presents a minimum at p_c which is lower for higher values of q and whose position shifts to higher p as q increases, as observed both in the numerical simulations [Fig. 3(b)] of the network with excitable and oscillatory elements and in the Ising network (Fig. 6). This means that, for values of p far from p_c—i.e., where $g\simeq 1$ [35]—the global dynamics is basically affected by only one positive eigenvalue. On the contrary, for values of p close to p_c, the global dynamics is affected not just by one, but several eigenvalues (the largest ones). Precisely, the contribution of the structure to the dynamical evolution can be described as

$$\mathbf{V}(t)=\sum_i e^{d\lambda_i^+ t}\mathbf{M}_i\mathbf{V}_0, \tag{5}$$

where $\mathbf{V}_0=\{V_1^0,V_2^0,\cdots,V_N^0\}$ is the vector of initial states and $\mathbf{M}_i$ are matrices independent of time. Thus, when $g\simeq 1$, $\mathbf{V}(t)\simeq e^{d\lambda^+ t}\mathbf{U}_0$, with $\mathbf{U}_0=\Sigma_i\mathbf{M}_i\mathbf{V}_0$ a linear combination of the initial states, indicating that the temporal evolution due to the structure is basically determined by one parameter, the eigenvalue λ^+. On the other hand, around p_c where g is smaller, more eigenvalues are needed to describe the effect of the structure, and as expressed by the Eq. (5), the system becomes more heterogeneous due to the connectivity.

Therefore, the intrinsic dynamics of the system is minimally constrained by the structure that arises around p_c due to the repulsive shortcuts.

V. DISCUSSION AND CONCLUSIONS

The results obtained above reflect the fact that at p_c there is a transition from a lattice with degree $k_i=2$ ($p=0$) to a lattice with degree $k_i=N-1$ ($p=1$). At p_c we have a SW whose degree distribution is of exponential type, indicating the presence of hubs, which is related to the existence of large eigenvalues in [36]. We also find that when hubs appear—i.e., when the dispersion of eigenvalues is large—the activity is enhanced. Since the MF corresponding to numerical simulations and the structure parameter g from spectral analysis are functions of p and q, it is possible to plot one versus the other as is done in Fig. 8. We observe that there is high activity for small values of g and low activity for larger g.

We can shed some light onto this discussion by regarding Fig. 9 in which the number N^+ of positive eigenvalues as a function of p and q is plotted. When $p\approx 0$, which essentially corresponds to a lattice, the initial oscillating units are unable to spread the activity throughout due to the fact that there are few positive eigenvalues. As $p\to 1$, shifting to a fully con-

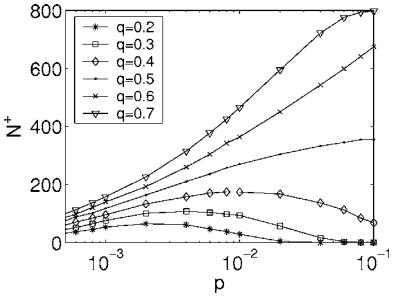

FIG. 9. Dependence of the number of λ_i^+, N^+, with the link probability p for different q values.

nected network, two different scenarios of low dispersion are possible. For values of q below 0.5, the number of λ_i^+ decreases and, as in the previous case, the modes associated with these few eigenvalues are not sufficient with activate the network. Alternatively, for $q>0.5$ there are many λ_i^+ but they are little dispersed. Since all dimensions in S^+ contribute similarly to the dynamics, nodes are indistinguishable from the view point of the topology (i.e., hubs disappear as p increases) and the dynamical units are constrained to evolve alike when they have different intrinsic dynamics.

On the contrary, if the dispersion is large, there is a balance between the intrinsic dynamics and the structure of the network. The topology close to p_c, due to the presence of phase-repulsive links, is such that the connectivity of the network is compatible with the diversity of the system.

In summary, we have shown numerically how a small fraction of phase-repulsive links can enhance activity and synchronization in a complex network of dynamical units. A spectral analysis allows us to obtain information about how the topology influences the dynamics. Around p_c, which is related to the topology, the presence of hubs with negative links makes it easier to spread the activity through the network. We have found that this activity is more coherent for the particular value of $q \approx 0.3$, indicating the existence of resonance.

ACKNOWLEDGMENTS

We thank J. R. Peláez for fruitful discussions. This work has been financially supported by the Spanish Ministry of Science and Technology under Project No. BFM2003-03081 and the URJC Project No. PPR2004-04. All numerical computations were performed at the Centro de Apoyo Tecnológico of the Universidad Rey Juan Carlos.

[1] D. J. Watts and S. H. Strogatz, Nature (London) **393**, 440 (1998).
[2] A.-L. Barabási and R. Albert, Science **286**, 509 (1999).
[3] D. J. Watts, *Small Worlds: The dynamics of networks between order and randomness* (Princeton University Press, Princeton, 1999).
[4] R. Albert and A.-L. Barabási, Rev. Mod. Phys. **74**, 47 (2002).
[5] S. N. Dorogovtsev and J. F. F. Mendes, Adv. Phys. **51**, 1079 (2002).
[6] S. Strogatz, Nature (London) **410**, 268 (2001).
[7] S. Boccaletti, V. Latora, Y. Moreno, M. Chavez, and D.-U. Hwang, Phys. Rep. **424**, 175 (2006).
[8] D. He, G. Hu, M. Zhan, W. Ren, and Z. Gao, Phys. Rev. E **65**, 055204(R) (2002).
[9] X. Wang, Y. Lu, M. Jiang, and Q. Ouyang, Phys. Rev. E **69**, 056223 (2004).
[10] L. F. Lago-Fernández, R. Huerta, F. Corbacho, and J. A. Sigüenza, Phys. Rev. Lett. **84**, 2758 (2000).
[11] M. Tinsley, J. Cui, F. V. Chirila, A. Taylor, S. Zhong, and K. Showalter, Phys. Rev. Lett. **95**, 038306 (2005).
[12] A. J. Steele, M. Tinsley, and K. Showalter, Chaos **16**, 015110 (2006).
[13] M. Kuperman and G. Abramson, Phys. Rev. Lett. **86**, 2909 (2001).
[14] M. Barahona and L. M. Pecora, Phys. Rev. Lett. **89**, 054101 (2002).
[15] T. Nishikawa, A. E. Motter, Y.-C. Lai, and F. C. Hoppensteadt, Phys. Rev. Lett. **91**, 014101 (2003).
[16] A. E. Motter, C. Zhou, and J. Kurths, Phys. Rev. E **71**, 016116 (2005).
[17] M. Chavez, C.-U. Hwang, A. Amann, H. G. E. Hentschel, and S. Boccaletti, Phys. Rev. Lett. **94**, 218701 (2005).
[18] I. Belykh, E. de Lange, and M. Hasler, Phys. Rev. Lett. **94**, 188101 (2005).
[19] L. Donetti, P. I. Hurtado, and M. A. Muñoz, Phys. Rev. Lett. **95**, 188701 (2005).
[20] M. I. Rabinovich, P. Varona, A. I. Selverston, and H. D. I. Abarbanel, Rev. Mod. Phys. **78**, 1213 (2006).
[21] P.-J. Kim, T.-W. Ko, H. Jeong, and H.-T. Moon, Phys. Rev. E **70**, 065201(R) (2004).
[22] I. Leyva, E. Allaria, S. Boccaletti, and F. T. Arecchi, Chaos **14**, 118 (2004).
[23] G. Balázsi, A. Cornell-Bell, A. B. Neiman, and F. Moss, Phys. Rev. E **64**, 041912 (2001).
[24] L. S. Tsimring, N. F. Rulkov, M. L. Larsen, and M. Gabbay, Phys. Rev. Lett. **95**, 014101 (2005).
[25] A. L. Hodgkin and A. F. Huxley, J. Physiol. (London) **117**, 500 (1952).
[26] Parameters: $C=1\ \mu\mathrm{F/cm^2}$, $g_{Na}=120\ \mathrm{mS/cm^2}$, $g_K=36\ \mathrm{mS/cm^2}$, $g_l=0.3\ \mathrm{mS/cm^2}$, $V_{Na}=50$ mV, $V_K=-77$ mV, $V_l=-54.4$ mV. Functions α_x and β_x with $x\in\{m,h,n\}$: $\alpha_m=0.1(V+40)/\{1-\exp[-(V+40)/10]\}$, $\beta_m=4\exp[-(V+65)/18]$, $\alpha_h=0.07\exp[-(V+65)/20]$, $\beta_h=1/\{1+\exp[-(V+35)/10]\}$, $\alpha_n=0.01(V+55)/\{1-\exp[-(V+55)/10]\}$, $\beta_n=0.125\exp[-(V+65)/80]$.
[27] G. Ermentrout and N. Kopell, SIAM J. Appl. Math. **54**, 478 (1994).
[28] G. Balázsi, A. Cornell-Bell, and F. Moss, Chaos **13**, 515 (2003).
[29] Although we use a SW network of Newman-Watts type (adding probability in a lattice) instead of a Watts-Strogatz network (rewiring probability), our results also apply to this latter case.

This is not only for theoretical reasons that prove that both SW networks are topologically equivalent for p small and N large [4], but because we have actually checked numerically that our findings on activity and synchronization are similar in both coupling schemes.

[30] H. Zhou and R. Lipowsky, Proc. Natl. Acad. Sci. U.S.A. **102**, 10052 (2005).

[31] T. Nishikawa and A. E. Motter, Phys. Rev. E **73**, 065106(R) (2006).

[32] G. Tanaka, B. Ibarz, M. A. F. Sanjuán, and K. Aihara, Chaos **16**, 013113 (2006).

[33] L. M. Pecora and T. L. Carroll, Phys. Rev. Lett. **80**, 2109 (1998).

[34] Curiously, although the Laplacian matrix is not symmetric and, in general, the resulting eigenvalues are expected to be complex, we have numerical evidence that they are always positive and negative real numbers for the range of p and q values explored.

[35] A value of g close to 1 is also possible for a set of a very dispersed positive eigenvalues, if all of them are very small. However, we have not found this case for the whole range of p and q considered.

[36] A. Arenas, A. Díaz-Guilera, and C. J. Pérez-Vicente, Phys. Rev. Lett. **96**, 114102 (2006).